Available online at www.sciencedirect.com

ScienceDirect

Journal of Differential Equations 380 (2024) 181–197

Journal of Differential Equations

www.elsevier.com/locate/jde

Critical periods in planar polynomial centers near a maximum number of cusps

Peter De Maesschalck [a,*], Joan Torregrosa [b,c]

[a] *Hasselt University, Campus Diepenbeek, Agoralaan Gebouw D, B-3590 Diepenbeek, Belgium*
[b] *Departament de Matemàtiques, Universitat Autònoma de Barcelona, 08193 Bellaterra, Barcelona, Spain*
[c] *Centre de Recerca Matemàtica, Campus de Bellaterra, 08193 Bellaterra, Barcelona, Spain*

Received 21 June 2023; accepted 18 October 2023
Available online 7 November 2023

Abstract

We provide the best lower bound for the number of critical periods of planar polynomial centers known up to now. The new lower bound is obtained in the Hamiltonian class and considering a single period annulus. This lower bound doubles the previous one from the literature, and we end up with at least $n^2 - 2$ (resp. $n^2 - 2n - 1$) critical periods for planar polynomial systems of odd (resp. even) degree n. Key idea is the perturbation of a vector field with many cusp equilibria, whose construction is by itself a nontrivial construction that uses elements of catastrophe theory.

MSC: primary 34C07; secondary 34C23, 37C27

Keywords: Critical periods; Hamiltonian vector fields; Best lower bound; Degree n vector field

1. Introduction

The study of the number of oscillations of the period function associated to a planar polynomial center has a long history that took a start with the seminal paper by Chicone and Jacobs in 1989 where the authors did a bifurcation analysis of the critical periods for planar vector fields in [2]. In classical Liénard families the isochronicity and monotonicity problems were studied

* Corresponding author.
E-mail addresses: peter.demaesschalck@uhasselt.be (P. De Maesschalck), joan.torregrosa@uab.cat (J. Torregrosa).

https://doi.org/10.1016/j.jde.2023.10.034
0022-0396/

in [12] and later in [4]. For polynomial families of arbitrary degree there are very few studies. The first lower bound of order n was obtained by Cima, Gasull, and Silva in 2008, see [3]. This result was quickly improved providing a lower bound of order $n^2/4$, using perturbations from a center as in [8], by Gasull, Liu, and Yang in a paper published in 2010, see [7]. More concretely, they proved that the number of critical periods is higher than or equal to $(n^2+6n-4)/4$ in the even degree case, with a similar but slightly worse bound for the odd degree case. This bound was recently improved by Cen in 2021, see [1]. Cen, with a very nice idea of removing cusps or fake saddles via a simple perturbation, provides a new lower bound, doubled in order. In fact, he proves that there exist odd degree Hamiltonian vector fields having a center for which the corresponding period function has at least $(n^2+2n-5)/2$ critical periods. Cen's construction leads for the even degree case to a slightly worse bound given by $(n^2-4)/2$. In both cases, the analyzed center has only one period annulus. In the present paper, inspired by Cen's idea, we managed to roughly double the number of oscillations. Providing a new lower bound of order n^2 instead of order $n^2/2$. Up to our knowledge, this is the best lower bound for the number of oscillations of the period function of a center, but we have no indications concerning the optimality of our result. The proof will closely follow Cen's proof but with a refined unfolding of a fake saddle into two cusps, as in [5]. Our main result is the following.

Theorem 1. *There exist (Hamiltonian) planar polynomial vector fields of odd (resp. even) degree $n \geq 3$, having a center and whose period function associated to the period annulus around that center has at least n^2-2 (resp. n^2-2n-1) critical periods.*

Remark 2. With *the* period function we mean the function T that maps a given Hamiltonian energy level h to the positive time it takes to travel along one round around the center, under condition that the level curve is homeomorphic to a circle. The Hamiltonian function in Theorem 1 is of degree $n+1$.

The key point is to study the period function associated to the center located at the origin of the planar polynomial vector field of degree $n=2m+1$ ($m \geq 1$), defined by the Hamiltonian

$$H_{a,b,\delta,\varepsilon}(x,y) = G_{a,\delta,\varepsilon}(x,y) + F_{b,\varepsilon}(y) = \int_0^x g_{a,\delta,\varepsilon}(s,y)ds + \int_0^y f_{b,\varepsilon}(s)ds, \tag{1}$$

where $\delta, \varepsilon > 0$ are sufficiently small parameters, $a=(a_1,\dots,a_m)$, $b=(b_1,\dots,b_m)$ satisfying $0<a_1<a_2<\cdots<a_m<1$, $0<b_1<b_2<\cdots<b_m<1$ and

$$f_{b,\varepsilon}(y) = y\prod_{i=1}^{m}((b_i-y)^2+\varepsilon), \quad g_{a,\delta,\varepsilon}(x,y) = x\prod_{i=1}^{m}((a_i-x+\delta y)^2+\varepsilon). \tag{2}$$

The construction involves making a particular choice for a and b. This idea is inspired by Cen's construction in [1], but unlike in that paper we use *a two-stage perturbation*: after analyzing $H_{a,b,0,0}$ in Section 2 we proceed to study the perturbation $H_{a,b,\delta,0}$ in Section 3 and finish the proof in the odd degree case in Section 4 by examining the effect of the ε-perturbation in $H_{a,b,\delta,\varepsilon}$. For the even degree case we will even need a third perturbation level; this is worked out in Section 5. Finally, we present an analytic example with an infinite number of oscillations in Section 6.

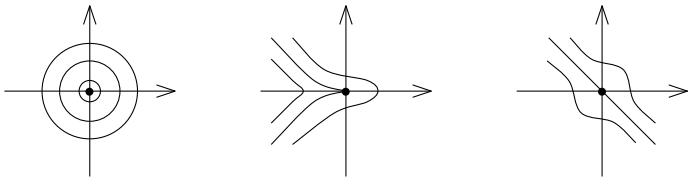

Fig. 1. Level curves of Hamiltonians in normal form coordinates near the equilibria that appear in this paper.

Three types of equilibria will play a role in the Hamiltonian systems here: we will relate them to critical points of Hamiltonian functions in local normal form coordinates:

(1) centers, i.e. where $H = u^2 + v^2$,
(2) cusps, i.e. where $H = u^3 + v^2$,
(3) fake saddles, i.e. where $H = u^3 + v^3$.

See Fig. 1 for the local phase portraits.

Remark 3. When considering the critical points of the Hamiltonians, their unfoldings are described by catastrophe theory (see for example [9]). The Hamiltonian $H = u^2 + v^2$ has a non-degenerate critical point (Morse type), which is stable. The Hamiltonian $H = u^3 + v^2$ is part of the stable unfolding $H_\lambda = u^3 + v^2 + \lambda u$ (fold catastrophe breaking up the associated cusp equilibrium into a saddle and a center). The Hamiltonian $H = u^3 + v^3$ is part of the stable unfolding $H_{\lambda,\mu,\nu} = u^3 + v^3 + \lambda u + \mu v + \nu uv$ (hyperbolic umbilic catastrophe). The unfolding contains regions where the equilibrium splits into two cusps; it is the basis of our construction. Using [9] one can see that the three above normal forms are 2-determined resp. 3-determined, where k-determinacy means it suffices to compare the k-order Taylor expansion of a given function with the normal form to conclude both are locally (right-)equivalent. (Note that right equivalence of two Hamiltonians corresponds to orbital equivalence of the associated vector fields.) Outside the Hamiltonian class, centers are of course not preserved under perturbation, cusps may undergo Bogdanov–Takens bifurcations, and fake saddles have a more involved unfolding; see [5].

Remark 4. A side result in this paper is the construction of degree n Hamiltonian vector fields with $O(n^2/2)$ cusps (see Proposition 12). It is in general not so easy to construct vector fields with prescribed equilibria and homoclinic/heteroclinic connections. The restriction to the Hamiltonian case makes the question a little bit more tractable, but it is still difficult. We remark in that light that looking for a Hamiltonian H with many cusps for the associated vector field is completely different from looking for an algebraic curve $H = 0$ with many cusps (as in [10]). See Fig. 6 for a phase portrait of a cubic system with a center and 4 cusps. It remains an open question whether or not the bound in Proposition 12 is optimal.

2. The initial unperturbed system

Although some of the results of this section can be seen in [1], for completeness we have reproduced the arguments here, at several places in a simpler way.

Clearly, for $\delta = \varepsilon = 0$, the differential system corresponding to the first integral $H_{a,b,0,0}(x, y)$, defined in (1), is

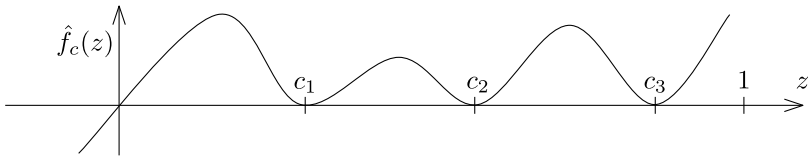

Fig. 2. Graph of function $\hat{f}_c$ (with $m = 3$); c can be either a or b.

$$\begin{aligned} \dot{x} &= -\hat{f}_b(y) = -y\prod_{i=1}^{m}(b_i - y)^2, \\ \dot{y} &= \hat{f}_a(x) = x\prod_{i=1}^{m}(a_i - x)^2. \end{aligned} \tag{3}$$

See Fig. 2 for graphs of $\hat{f}_a$, $\hat{f}_b$. The origin is an equilibrium; we will refer to it as $(a_0, b_0) := (0, 0)$, and consider it together with the indexed sequence of points (a_i, b_j):

Lemma 5. *The equilibrium points of system* (3) *are located at* (a_i, b_j)*, for* $i, j = 0, \ldots, m$ *and the qualitative behavior is of the following type:*

(i) $(0, 0)$ *is a non-degenerate center and the algebraic intersection multiplicity of the two nullclines is* 1*;*
(ii) $(a_i, 0)$ *and* $(0, b_i)$*, for* $i = 1, \ldots, m$ *are cusps and the algebraic intersection multiplicity of the two nullclines is* 2*; and*
(iii) (a_i, b_j) *for* $i, j = 1, \ldots, m$ *are fake saddles and the algebraic intersection multiplicity of the two nullclines is* 4*.*

Proof. The proof follows just computing the first and second derivatives of the function $\hat{f}_c$ defined in (3) and their values at $z = c_i$ for each i.

When $c_i \neq c_j$, the function $\hat{f}_c(z)$ has a simple zero at $z = 0$ and double zeros at $z = c_i$, for $i = 1, \ldots, m$. (See also Fig. 2). This observation directly leads to the claims on the algebraic intersection multiplicity. (See e.g. [6] for background on algebraic multiplicity.)

Following Remark 3, it suffices to compute the Taylor expansion of $H_{a,b,0,0}$ at the various equilibria, and the relate them to one of the normal forms listed above that remark by means of a simple linear transformation. This is in all the cases an elementary task: using the expressions for $\hat{f}_a(x)$ and $\hat{f}_b(y)$ we easily find the Taylor expansions:

(1) Around $(0, 0)$ we have $H_{a,b,0,0} = \frac{x^2}{2}\alpha + \frac{y^2}{2}\beta + O(x^3) + O(y^3)$ so a suitable transformation $(u, v) = (\tilde{\alpha}x, \tilde{\beta}y)$ puts the 2-jet in normal form. We point out to the reader that the shape of the Hamiltonian for $(\delta, \varepsilon) = (0, 0)$ is particular in the sense that the variables are separated. It facilitates the transformation to normal form: this transformation is a combination of two scalar diffeomorphisms, one for transforming x and one for transforming y. It is why we wrote the remainder terms as $O(x^3) + O(y^3)$ instead of the slightly weaker $O(\|(x, y)\|^3)$. This remark will be valid for the expressions below as well.

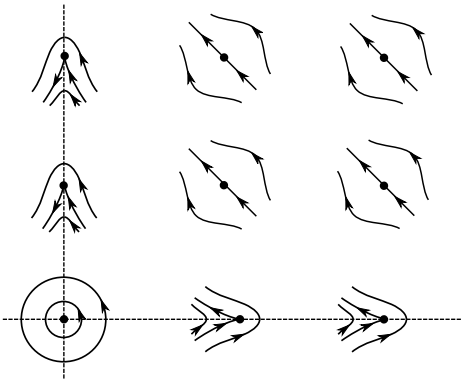

Fig. 3. Qualitative behavior near the equilibria.

(2) Around $(a_i, 0)$ (for $i \geq 1$) we have $H_{a,b,0,0} = h_{i0} + \frac{(x-a_i)^3}{3}\alpha + \frac{y^2}{2}\beta + O((x-a_i)^4) + O(y^3)$ for some positive constants α, β. So a suitable transformation $(u, v) = (\tilde{\alpha}(x-a_i), \tilde{\beta}y + \gamma y^2)$ puts the 3-jet in normal form.
(3) Around $(0, b_j)$ (for $j \geq 1$) we have $H_{a,b,0,0} = h_{0j} + \frac{x^2}{2}\alpha + \frac{(y-b_j)^3}{3}\beta + O(x^3) + O((y-b_j)^4)$ for some positive constants α, β. So a suitable transformation $(u, v) = (\tilde{\alpha}(y-b_k), \tilde{\beta}x + \gamma x^2)$ puts the 3-jet in normal form.
(4) Similarly for the equilibria (a_i, b_j) with $i \geq 1$ and $j \geq 1$.

Taking into account the different local changes of coordinates, we arrive at a partially complete understanding of the phase portrait: see Fig. 3 for the local qualitative behavior of the equilibria. □

Lemma 6. *When $a = b$ and $(\delta, \varepsilon) = (0, 0)$, the vector field (3) associated to the Hamiltonian (1) is time-reversible with respect the straight line $y - x = 0$.*

Proof. Applying the transformation $(x, y, t) \mapsto (y, x, -t)$ (which is a time reversal combined with the orthogonal reflection about $y = x$) leaves the vector field invariant when $a = b$. □

Lemma 7. *Consider the Poincaré compactification of the polynomial vector field (3) on the Poincaré disc. The circle at infinity of (3) has no equilibria; in other words, (3) has a center at infinity.*

Proof. One can use the fact that the phase portrait near infinity only depends on the terms of highest degree of (3), which is seen in $(\dot{x}, \dot{y}) = (\cdots - \alpha y^{2m+1}, \cdots + \alpha x^{2m+1})$ for some positive constant α. There are no equilibria because $\dot{y}x - \dot{x}y = \cdots + \alpha(x^{2m+2} + y^{2m+2})$, which reveals that the part of $\dot{\theta}$ in polar coordinates that is dominant near $r = \infty$ is strictly positive. □

In the following lemma we describe some interesting properties of the *singular level curves*, i.e. those levels containing equilibria, and we obtain a better description of how these singular level curves are positioned relative to each other.

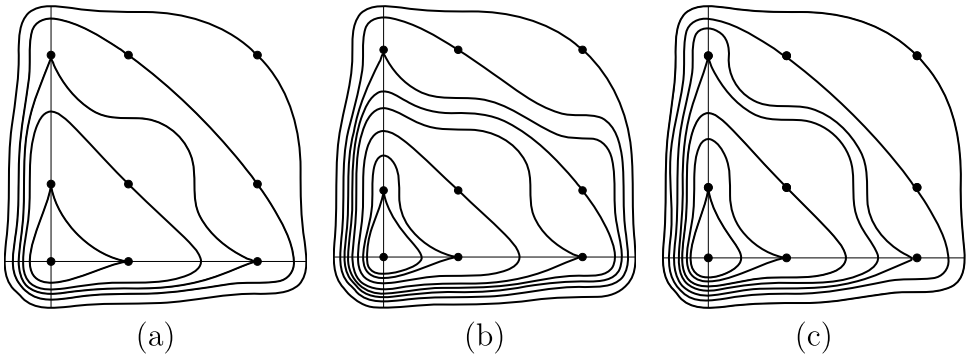

Fig. 4. Possible configurations of the level curves passing through the cusp and fake saddles. (a) A symmetric configuration. (b) A generic non-symmetric configuration without heteroclinics. (c) A non-generic non-symmetric configuration with one heteroclinic.

Lemma 8. *Consider the Hamiltonian $H = H_{a,b,0,0}$, and the levels $h_{ij} = H(a_i, b_j)$ at the various equilibria listed in Lemma 5.*

(1) The sequence $(h_{ij})_{i=0,\dots,m}$ is a strictly increasing sequence for each j, and $(h_{ij})_{j=0,\dots,m}$ is a strictly increasing sequence for each i. Furthermore, when $a = b$ then $h_{ij} = h_{ji}$ for all i, j.
(2) The set of (a, b) for which all singular levels h_{ij} are pairwise distinct from each other is dense inside the whole parameter space.
(3) Choose a, b in the above dense set. The singular levels h_{ij}, for $(i, j) \neq (0, 0)$, have level curves that are homeomorphic to a circle and that surround the center at the origin. Outside the singular level curves the phase plane is filled with periodic orbits around the center. See Fig. 4 for a possible configuration of them.

Proof. The first statement follows directly from the definition of functions $\hat{F}_{a,b}$ defined in the proof of Lemma 5 and the fact that all a_i and b_j are positive. The statement concerning the symmetric case $a = b$ follows directly from the symmetry provided by Lemma 6.

For the second statement, consider, for a fixed $i \geq 1$, the map

$$\tilde{F}_{ik} \colon a_i \mapsto \int_0^{a_k} f_a(x)dx = F_a(a_k),$$

hereby focusing on the variation of a single parameter a_i. Then observe that when $k \neq i$ the expression $\tilde{F}_{ik}(a_i)$ is a quadratic polynomial in a_i of degree 2. On the other hand when $k = i$ the expression has a strictly positive third order derivative: $\tilde{F}'''_{ii} = f''_a(a_i) > 0$. It implies that the map

$$a_i \mapsto h_{ij} - h_{k\ell}$$

is not identically zero when $i \neq k$. Similarly $b_j \mapsto h_{ij} - h_{k\ell}$ is not identically zero when $j \neq \ell$. A fortiori the map that considers all parameters and that sends $(a, b) \mapsto (h_{ij} - h_{k\ell})$ is never identically zero when $(i, j) \neq (k, \ell)$. So the set in parameter space where one or more levels are the same is a finite union of algebraic hypersurfaces, hence (now following Cen's argument) the complement is open and dense.

Let us finally deal with the third part. The absence of equilibria at infinity obtained in Lemma 7 is not so unimportant: it shows there are no unbounded level curves, or more concretely: it shows that any separatrix (of any of the cusps or fake saddles) must connect to another one of these separatrices (to form a homoclinic or heteroclinic connection). If we however take all singular levels pairwise distinct, then no heteroclinics appear and the cusps and fake saddles are part of homoclinic loops. By looking at the signs of $\dot{x}$ and $\dot{y}$ in the four quadrants one concludes that all these loops circle around the origin. □

Remark 9. The way that cusps alternate with fake saddles, when ordering the different singular points by increasing energy value, defines the qualitative picture. Different configurations lead to pictures that are completely different from those shown in Fig. 4. It is for example possible to have all heteroclinic cusp connections inside the heteroclinic or homoclinic fake saddle connections (this appears just taking all a_i and, symmetrically, all b_i close enough). The precise configuration is however not important in view of proving our results. All we need is that the homoclinics are nested in each other, as stated in Lemma 8.

Lemma 10. *The period function $T(h)$ along the level curves $\Gamma_h = \{H_{a,b,0,0} = h\}$ corresponding to non-singular energy levels h tend to infinity as h approaches one of the singular energy levels $h_{ij} \neq 0$. In other words the graph of T has vertical asymptotes at $h = h_{ij}$.*

Proof. Integration time tends to infinity as one approaches equilibrium on a singular level curve (except at the center). Note that there is no need of computing precise asymptotics (like for example in [11]) in view of proving our results. □

Let us now describe the qualitative behavior of the period function for the unperturbed system. For completeness, note that the period function near the linear center for $(\delta, \varepsilon) = (0, 0)$ can be easily obtained using polar coordinates. We define

$$T_0 = \frac{2\pi}{(\prod_{i\geq 1} a_i)(\prod_{j\geq 1} b_j)} > 0.$$

Then:

Corollary 11. *There exist values of a and b (and keeping $(\delta, \varepsilon) = (0, 0)$) such that the period function associated to (3) has $m^2 + 2m$ asymptotes. Moreover, the period $T(h)$ tends to T_0 as $h \to 0$ and tends to 0 as $h \to \infty$. See Fig. 5 for a typical graph.*

Proof. The first statement follows from Lemma 10 and counting the number of equilibria we have exactly $m^2 + 2m$ of them. The limiting behavior of the period function near the center has been briefly discussed above. In the proof of Lemma 7 we have computed $r^2\dot{\theta} = \dot{y}x - \dot{x}y = \cdots + \alpha(x^{2m+2} + y^{2m+2})$. Hence, when r goes to infinity the period of the center located at infinity goes to zero. □

3. The first perturbation. From fake saddles to cusps

This section picks up the main differences of our work with [1]. In this section we will consider, as in the previous section, only odd degree n.

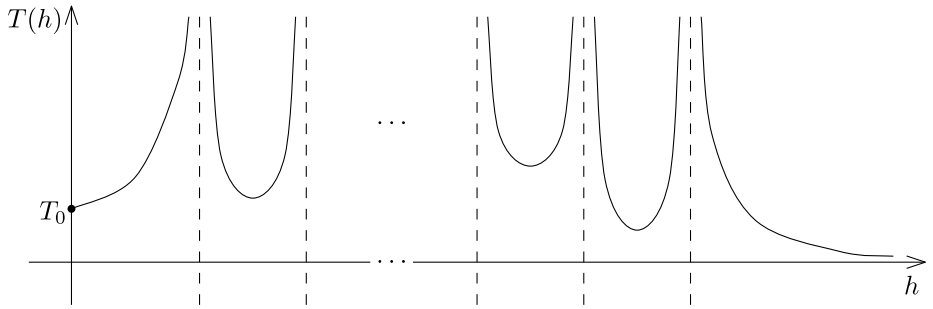

Fig. 5. Graph of the period function for the unperturbed ($\delta = \varepsilon = 0$) system.

Our aim is to perturb the Hamiltonian $H_{a,b,0,0}$ in a way that the existing center and cusps remain but the existing fake saddle breaks into two cusps. Referring to Remark 3 we will have to take care that none of the existing cusps break into a saddle and a center.

Clearly, for $\varepsilon = 0$, the differential system corresponding to the first integral $H_{a,b,\delta,0}(x, y)$, defined in (1), is

$$\begin{aligned} \dot{x} &= -\int_0^x \frac{\partial g_{a,\delta,0}(s,y)}{\partial y}\, ds - y\prod_{i=1}^{m}(b_i - y)^2, \\ \dot{y} &= x\prod_{i=1}^{m}(a_i - x + \delta y)^2. \end{aligned} \tag{4}$$

Proposition 12. *There exist values of (a, b, δ), such that system (4) (keeping $\varepsilon = 0$) has an equilibrium of center type at $(0, 0)$ and $2m^2 + 2m$ equilibria of cusp type. There are no other equilibria. Moreover, the energy levels are different for each of the equilibrium points.*

The proof is somewhat long; before initiating it let us give some insights. In Lemma 5 the characterization of equilibria was principally based on the intersection number of the two nullclines. The nullclines were horizontal and vertical there, see Fig. 6 for the lowest degree case, i.e. the cubic case. If we want to make sure the cusps on the two principal axes are not broken, but the other ones have to, then the nullclines have to change in a specific way: we refer to Fig. 6 for the way that we do it: the order 4 intersections are split in two order 2 intersections, but the existing order 2 intersections are not being split. We also show in Fig. 6 the level curves through the equilibria, to give an impression of the phase portraits before and after perturbation.

Proof of Proposition 12. The proof will follow studying the local phase portrait of each equilibrium depending on where it is located, at the origin, on the y-axis, near the x-axis, or far from the coordinates axis. Equivalently, we will prove that the local algebraic multiplicity of the intersection of the components of (4) is always 2 except at the origin which is 1. More concretely, the equilibria near the coordinate axis, except the origin, remains double, as the case with $\delta = 0$, while the rest, which are of multiplicity 4 when $\delta = 0$, split exactly in two double points.

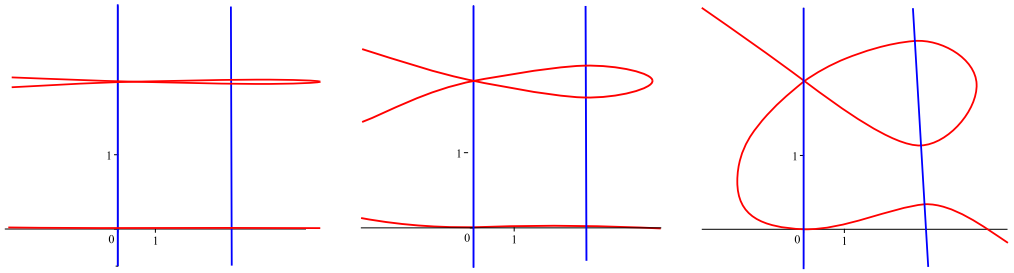

Fig. 6. Cubic case. Nullclines of the vector field for values of different values of $\delta < 0$, ordered by increasing distance to $\delta = 0$. In red (blue) we have drawn when the vector field has vertical (horizontal) direction.

From the definitions in (2) it is clear that $(0, 0)$ is an equilibrium point of (4) and, as the perturbation by δ does not break the Hamiltonian character, the local phase portrait given in Lemma 5 remains. So, the origin is of center type. In particular, the local multiplicity is 1.

On the y-axis, the equilibria remain located at $(0, b_j)$ and again, as in the previous case, the phase portrait given in Lemma 5 does not change: they are all of cusp type and with local multiplicity 2. Another way of seeing this is to observe that the local expression of H, which was given before perturbation by

$$H_{a,b,0,0} = h_{0j} + \frac{x^2}{2}\alpha + \frac{(y-b_j)^3}{3}\beta + O(x^3) + O((y-b_j)^4),$$

for some positive constants α, β (see Lemma 5), perturbs in an $O(\delta x^2)$-way. To see this notice that $g_{a,\delta,0}(x, y) = g_{a,0,0}(x, y) + \delta x r(x, y)$ for some $r(x, y)$ implying that $G_{a,\delta,0}(x, y) = G_{a,0,0}(x, y) + \delta x^2 R(x, y)$ for some $R(x, y)$. So we find

$$\begin{aligned} H_{a,b,\delta,0} &= h_{0j} + \frac{x^2}{2}\alpha + \frac{(y-b_j)^3}{3}\beta + \delta x^2 R(x, y) + O(x^3) + O((y-b_j)^4) \\ &= h_{0j} + \frac{x^2}{2}(\alpha + O(\delta, x)) + \frac{(y-b_j)^3}{3}\beta + O((y-b_j)^4) \\ &= h_{0j} + \frac{1}{2}\left(x\sqrt{\alpha + O(\delta, x)}\right)^2 + \frac{1}{3}\left((y-b_j)\sqrt[3]{\beta + O(y-b_j)}\right)^3, \end{aligned}$$

Like in the proof of Lemma 5, an obvious transformation puts the 3-jet in cusp normal form, which is sufficient to prove the cusp behavior.

Let us next focus on the cusps on x-axis, i.e. located at $(a_i, 0)$. Our argument that they perturb to cusps is based solely on the study of the two nearby nullclines. The $\dot{y} = 0$ nullcline is actually a double line $x = a_i + \delta$, which is almost vertical for small $\delta \neq 0$. The other nullcline is more involved, but we only need $\dot{x} = \beta y + O(y^2) + O(\delta)$ to know, using the Implicit Function Theorem, that near $(a_i, 0)$ the nullcline is a smooth graph $y = \delta\phi(x, \delta)$. Clearly there is a unique intersection point near $(a_i, 0)$, and it is automatically a double point. In the Hamiltonian framework, this implies that the perturbed equilibrium is necessarily a cusp (it is an easy consequence of catastrophe theory).

The other equilibria are again located at straight lines $x = a_i + \delta y$, and are close to the fake saddles (a_i, b_j) if we keep δ close to 0. Again, any of these perturbed equilibria are at least

double points, because of the specific form of the nullcline $\dot{y} = 0$ of (4). Using Lemma 13 stated below, it hence suffices to show that the nullcline $\dot{x} = 0$ of (4) bifurcates from a double line $y = b_j$ into two separate curves near the point (a_i, b_j).

We recall the expression for $\dot{x}$, stressing its dependence on (y, δ), and keeping the dependence on x silent:

$$\dot{x} = \varphi(y, \delta) = \psi(y, \delta) + \phi(y)$$

with

$$\psi(y, \delta) = \int_0^x \left(\frac{\partial}{\partial y} s \prod_{k=1}^{m} (a_k - s + \delta y)^2 \right) ds,$$

and

$$\phi(y) = y \prod_{k=1}^{m} (b_k - y)^2.$$

Fixing $i \geq 1$ and $j \geq 1$ we immediately see that

$$\phi(y) = (b_j - y)^2 (\underbrace{b_j \textstyle\prod_{k=1}^{m} (b_k - b_j)^2}_{\geq 0} + O(y - b_j)).$$

Straightforward computations show that

$$\begin{aligned} \frac{\partial}{\partial y} s \prod_{k=1}^{m} (a_k - s + \delta y)^2 \Big|_{y = b_j + \alpha} &= s \sum_{k=1}^{m} 2(a_j - s + \delta y) \delta \prod_{\substack{\ell=1 \\ \ell \neq k}}^{m} (a_\ell - s + \delta y)^2 \\ &= \Big(s \sum_{k=1}^{m} 2(a_j - s) \prod_{\substack{\ell=1 \\ \ell \neq k}}^{m} (a_\ell - s)^2 \Big) \delta + \cdots \end{aligned}$$

so

$$\psi(\alpha, \delta) = \delta(\psi_1 + O(y - b_j, \delta)),$$

with

$$\psi_1 := 2 b_j \int_0^x \Big(s \sum_{k=1}^{m} 2(a_j - s) \prod_{\substack{\ell=1 \\ \ell \neq k}}^{m} (a_\ell - s)^2 \Big) ds.$$

Assuming $\psi_1 = \psi_1(x)$ is strictly positive near $x = a_i$, the nullcline is given by

$$\delta(\psi_1 + \cdots) + (y - b_j)^2 (\phi_1 + \cdots) = 0 \tag{5}$$

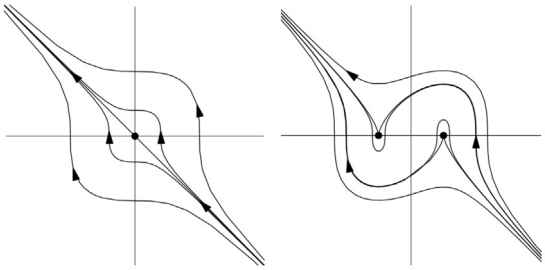

Fig. 7. From a fake saddle to two cusps.

which would prove the unfolding of the double line $y = b_j$ into two nearby curves for $\delta < 0$ sufficiently close to 0.

An easy way to see that there exists values of a_j such that $\psi_1 > 0$ is to take all very close to the same value A. We can substitute $x = a_i = a_j = a_\ell = A$ in the above first term and, at the limit point, we get

$$\begin{aligned}\psi_1^A &= \int_0^A \Big(s \sum_{k=1}^{m} 2(A-s) \prod_{\substack{\ell=1 \\ \ell \neq k}}^{m} (A-s)^2\Big) ds \\ &= 2m \int_0^A s(A-s)^{2m-1} ds \\ &= \frac{A^{2m+1}}{2m+1} > 0.\end{aligned}$$

Consequently, for nearby choices of $a = (a_1, \ldots, a_m)$ the property on ψ_1 remains valid. In fact using the density property in Lemma 8 we can additionally assume that all energy levels of the unperturbed equilibria at $\delta = 0$ are distinct for the chosen set of parameters (a, b). It then follows, using Lemma 13 below, the presence of two nearby cusps at different energy levels for $\delta < 0$ sufficiently small. Note that it is immediately clear from (5) that there are no equilibria perturbing from the fake saddles when $\delta > 0$. □

As announced inside the proof of Proposition 12, we state and prove following lemma:

Lemma 13. *Let $H = x^3 + y^3 + \lambda x + \mu y + \nu xy$. If the associated planar vector field does not have hyperbolic equilibria, then either there is no equilibrium at all, or there is a fake saddle equilibrium (and then $(\lambda, \mu, \nu) = (0, 0, 0)$), or there are two cusp equilibria, and in that case the values of H of both levels are distinct, see Fig. 7 for an example.*

Proof. The number of equilibria, taken multiplicity into account, of the complexified system is 4, so when there are no multiplicity 1 equilibria, we find only the following possibilities: 0 real equilibria, 2 real equilibria of multiplicity 2, and 1 equilibrium of multiplicity 4. It is not so hard to show that the last case only occurs for $(\lambda, \mu, \nu) = (0, 0, 0)$, and one can also see that the second case only occurs for $(\lambda, \mu, \nu) = (s, 0, 0)$ or $(\lambda, \mu, \nu) = (0, s, 0)$, for some $s < 0$. The two possibilities are the same upon exchanging x and y, so let us focus on the first one. Then

$$H = x^3 + sx + y^3.$$

The two equilibria are located at $x = \pm\sqrt{-s/3}$, $y = 0$, which surely have different energy levels. □

Like in the previous section, we could study infinity and rule out the possibility of equilibria there, thus showing that all level sets, singular and non-singular ones, are homoclinic connections and periodic orbits around the origin. We again finish the section by describing the qualitative behavior of the graph of the period function for $\varepsilon = 0$. It is similar to the one for $\delta = \varepsilon = 0$, i.e. Fig. 5 remains valid also for $\delta \neq 0$, but with more asymptotes.

Corollary 14. *Let $(a, b, \delta, \varepsilon = 0)$ be like in Proposition 12. Then the period function associated to (3) has $2m^2 + 2m$ asymptotes. Moreover, the behavior near $h = 0$ and near $h = \infty$ is similar to the unperturbed case.*

We finish this section by giving a supplementary explicit example in the cubics (e.g. with degree 4 Hamiltonian), for which it is elementary to show (ideally with the aid of some computer algebra program), for a specific value of δ, the claims that are only proven to be correct in the above proposition for $\delta < 0$ sufficiently close to 0. It is in fact this family that we used as input for Fig. 6. Of course, for the remainder of the proof of our main theorem, the reader may continue to read the next section.

Taking $m = 1$ and using $f_{2,\varepsilon}(x) = y((2-y)^2 + \varepsilon)$ and $g_{3,\delta,\varepsilon}(x, y) = x((3 - x + \delta y)^2 + \varepsilon)$ we get the specific degree 4 Hamiltonian

$$\begin{aligned} H_{3,2,\delta,\varepsilon} = {} & \tfrac{1}{4}x^4 - \tfrac{2\delta}{3}x^3 y + \tfrac{\delta^2}{2}x^2 y^2 + \tfrac{1}{4}y^4 \\ & - 2x^3 + 3\delta x^2 y - \tfrac{4}{3}y^3 + \tfrac{9}{2}x^2 + 2y^2 + \varepsilon\tfrac{x^2+y^2}{2}. \end{aligned} \tag{6}$$

For $(\delta, \varepsilon) = (-1/9, 0)$ it corresponds to the following cubic vector field:

$$\begin{aligned} \dot{x} &= -\tfrac{2}{27}x^3 - \tfrac{1}{81}x^2 y - y^3 + \tfrac{1}{3}x^2 + 4y^2 - 4y, \\ \dot{y} &= \tfrac{1}{81}x\,(9x + y - 27)^2. \end{aligned}$$

It has 5 equilibrium points $P_0 = (0, 0)$, $P_1 = (0, 2)$, $P_2 = \left(\frac{225}{76}, \frac{27}{76}\right)$, and $P_\pm = (3 - 3\gamma_\pm, 27\gamma_\pm)$, where $\gamma_\pm = \frac{5}{74} \pm \frac{3}{518}\sqrt{21}$. In Table 1 we list the local normalizing transformations and resulting normal forms of the Hamiltonian up to order 3. Clearly P_0 is a center and the other four are cusp points.

The plots of the nullclines of the vector field corresponding to H_δ, for $\delta = -10^{-4}, -10^{-2}, -1/9$, are shown in Fig. 6. For the sake of completeness we show the phase portrait of the vector field with $\delta = -1/9$ in Fig. 8.

4. The second perturbation. Removing equilibria

In this section we will prove Theorem 1 for odd degree n as a direct consequence of the results proved in Section 3. As we have described above, for $\delta < 0$ and $\varepsilon > 0$, the differential system corresponding to the Hamiltonian $H_{a,\delta,\varepsilon}(x, y)$, defined in (1), is

Table 1
Normalizing transformations (up to order 3) near equilibria of a cubic example.

P	Transformation	Local normal form of $H_{-1/9}$
P_0	$x = u + \frac{2}{9}u^2$ $y = v + \frac{1}{12}u^2 + \frac{1}{3}v^2$	$H_0 = \frac{9}{2}u^2 + 2v^2$
P_1	$x = u + \frac{6}{25}u^2 + \frac{1}{25}uv$ $y = 2 + v$	$H_1 = \frac{4}{3} + \frac{625}{162}u^2 + \frac{2}{35}v^3$
P_2	$x = \frac{225}{76} + u - \frac{1}{9}v$ $y = \frac{27}{76} + v + \frac{18088}{30375}v^2$	$H_2 = \frac{11585997}{1755904} + \frac{125}{152}v^2 + \frac{75}{76}u^3$
$P_\pm$	$x = 3 - 3\gamma_\pm$ $y = 27\gamma_\pm + v + \frac{1-\gamma_\pm}{13-238\gamma_\pm}u^2$ $+ \frac{1-\gamma_\pm}{117-2142\gamma_\pm}uv - \frac{4-81\gamma_\pm}{13-238\gamma_\pm}v^2$	$H_\pm = \frac{279207}{38332} - \frac{37179}{2738}\gamma_\pm$ $+ \frac{238\gamma_\pm - 13}{6}v^2$ $+ (1-\gamma_\pm)u^3$

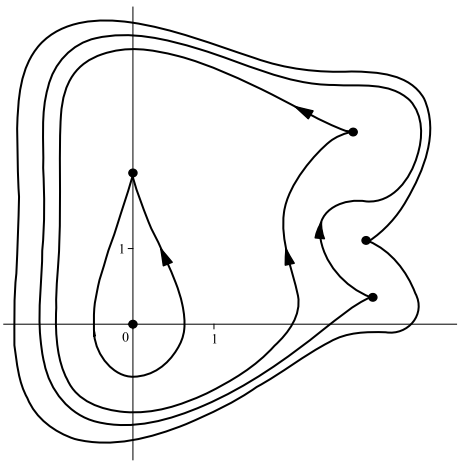

Fig. 8. Qualitative phase portrait of an explicit cubic system with one center and three cusps.

$$\begin{aligned} \dot{x} &= -\int_0^x \frac{\partial g_{a,\delta,\varepsilon}(s,y)}{\partial y}\,ds - y\prod_{i=1}^{m}((b_i-y)^2+\varepsilon), \\ \dot{y} &= x\prod_{i=1}^{m}((a_i-x+\delta y)^2+\varepsilon). \end{aligned} \tag{7}$$

As in [1], when $\varepsilon > 0$ small enough, the equilibria located out of the origin disappear and all asymptotes of the period function provided by Corollary 14 are replaced by maxima of the corresponding period function. Consequently, we have $2m^2+2m$ maxima and $2m^2+2m-1$ minima. Hence, as $n = 2m+1$, we obtain at least $4m^2+4m-1 = n^2-2$ critical periods.

Remark 15. If we want to be more precise then we say that for any orbit $\gamma_{a,b,\delta,\varepsilon}$ that approaches a singular level curve $\gamma_{a,b,\delta,0}$ the period tends to ∞, whereas the period function remains bounded as $\varepsilon \to 0$ for orbits that are away from the singular level sets. Since we have a finite number of singular levels, we can take $\varepsilon > 0$ small enough for the period function to have the guaranteed minimum number of oscillations. This more precise explanation shows that some care is needed when one wants to generalize the results to constructing examples with an infinite number of critical periods.

5. The third perturbation. Near infinity

This section is devoted to the proof of the second part of Theorem 1, that is when the degree of the vector field n is even. Our approach differs substantially from the one in [1]. We will use again a perturbative mechanism, now of system (7).

Let us consider Hamiltonian system of degree $n = 2m + 2$ given by

$$\dot{x} = -\int_0^x \frac{\partial g_{a,\delta,\varepsilon}(s,y)}{\partial y}\, ds - y\prod_{i=1}^{m}((b_i - y)^2 + \varepsilon) + \mu y^{2m+2},$$
$$\dot{y} = x\prod_{i=1}^{m}((a_i - x + \delta y)^2 + \varepsilon) - \mu x^{2m+2}.$$

where μ is a small parameter. It corresponds to the Hamiltonian

$$\tilde{H}_{a,b,\delta,\varepsilon,\mu} = H_{a,b,\delta,\varepsilon} - \frac{\mu}{2m+3}\left(x^{2m+3} + y^{2m+3}\right).$$

When $\mu = 0$ all the results proved in previous section apply, and it is easy to check that all the equilibria bifurcations and oscillations of the period function occurs in a compact region K. Consequently, for μ small enough, the number of oscillations of the period function remains as for the odd Hamiltonian of odd degree $2m + 1$. Therefore, the proof for even degree finishes because the number of oscillations will be, using Theorem 1 for the odd degree case, at least $(2m + 1)^2 - 2 = n^2 - 2n - 1$.

Remark 16. The above proof does not depend on the explicit perturbation terms. But if we would like to improve the lower bound a little (only one extra oscillation), we suggest taking the next steps, that we leave for the reader to verify. When $\mu \gtrless 0$, there are exactly two nodes at infinity, located in the direction of $y + x = 0$. This is because $\dot{y}x - \dot{x}y = \cdots - \mu(x^{2m+3} + y^{2m+3})$. The fact that they are nodes should be easy to prove. Additionally, from infinity emerge two (finite) saddles from the positive y-axis and another from the positive x-axis. Finally, one observes an additional center equilibrium in the direction $y - x = 0$ for x, y big enough. A summary is shown in Fig. 9. By considering this perturbation, the period annulus has a boundary defined by a heteroclinic cycle, partly along infinity and also containing a heteroclinic saddle connection between two hyperbolic saddles in the finite region. The period function should hence go to infinity as one approaches this singular cycle, so an extra oscillation occurs.

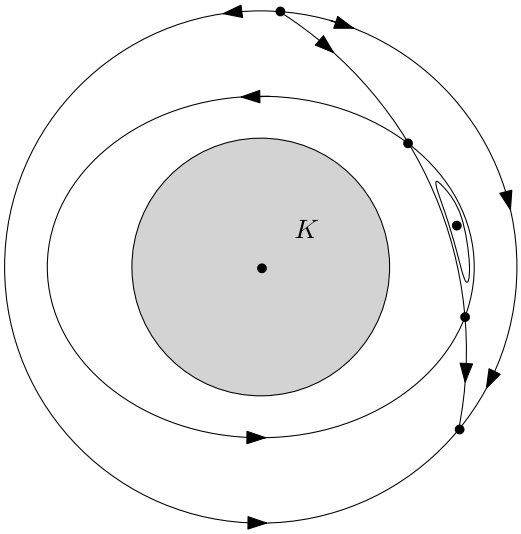

Fig. 9. Phase portrait on the Poincaré sphere after the third perturbation. The dynamics in the compact region K does not change qualitatively under this final perturbation.

6. No upper bound for analytic Hamiltonian vector fields

Finally, we will extend this idea to an analytic vector field that the unperturbed system, taking $\varepsilon = 0$, has infinitely many degenerate equilibrium points but the presented proof does not provide infinitely many isolated critical periods. Nevertheless, at the end of this section we present a simple ad-hoc example of an analytic vector field with infinitely many critical periods, unrelated to any nearby cusp equilibria.

Proposition 17. *For any n, there exist $\varepsilon > 0$ small enough such that the period function of system*

$$\begin{aligned} \dot{x} &= -y(1+\varepsilon-\sin y),\\ \dot{y} &= x(1+\varepsilon-\sin x), \end{aligned} \tag{8}$$

has at least n critical periods.

Proof. The proof follows the same steps as the proof of Theorem 1. We start describing the phase portrait of the unperturbed system (8) when $\varepsilon = 0$. It has only one non-degenerate center located the origin and the other equilibrium points are of cusp and fake saddle type. The cusps are located at $(0, \pi/2 + 2k\pi)$ and $(\pi/2 + 2k\pi, 0)$, for any $k \in \mathbb{Z}$ and the fake saddles are located at $(\pi/2 + 2k\pi, \pi/2 + 2\ell\pi)$, for any $k, \ell \in \mathbb{Z}$. Here we have no other centers nor saddles. This system is also time reversible with respect to the straight line $y - x = 0$. Consequently, we have only one period annulus and the period function has infinitely many of asymptotics and minima. The proof finishes taking $\varepsilon > 0$ small enough and, by continuity, the asymptotics disappear converting to maxima and the number of minima remain. We note that for a fixed ε we can control only the oscillations in a compact region. Of course decreasing ε the number of oscillations increases and the compact region can be taken higher. But we can not extend this argument to prove the

existence of infinitely many of critical periods because we have not described the behavior of infinity and the uniformity of the decreasing of ε. □

We remark that in equation (8) also the value of the energy levels decrease along vertical and horizontal straight lines and we do not need to study if in a level there are one or more equilibria because there are infinitely many of them. In fact, the qualitative behavior of this example is very close to the odd degree study made by Cen in [1]. Clearly, there are other analytic vector fields having the same property, a similar result can be found changing the function $1 - \sin y$ by $\cos^2 y$.

Finally, if we fix the compact the number of oscillations can be increased increasing the frequency of oscillations, $1 - \sin ky$, but fixed ε the finiteness is maintained. Hence, this approach does not prove that we have "infinitely many" isolated critical periods.

As mentioned in the beginning of this section we now present a simple example of a Hamiltonian vector field with infinitely many cusps: consider

$$H_\varepsilon(x, y) = x^2 + y^2 + \varepsilon \sin(x^2 + y^2), \qquad 0 < \varepsilon < 1.$$

We write $H_\varepsilon(r\cos\theta, r\sin\theta) = \tilde{H}_\varepsilon(r, \theta)$ in order to consider H_ε in polar coordinates:

$$\tilde{H}_\varepsilon(r, \theta) = r^2 + \varepsilon \sin(r^2),$$

so we immediately find the associated family of vector fields in polar coordinates:

$$\dot{r} = -\frac{1}{r}\frac{\partial \tilde{H}_\varepsilon}{\partial \theta} = 0, \qquad \dot{\theta} = \frac{1}{r}\frac{\partial \tilde{H}_\varepsilon}{\partial r} = 2 + 2\varepsilon\cos(r^2).$$

When $0 < \varepsilon < 1$, all orbits are circles $r = r_0$. Recall that we use the energy level as a parameter for the orbits (see Remark 2), so we find

$$T_\varepsilon(r_0^2 + \varepsilon \sin(r_0^2)) = \frac{\pi}{1 + \varepsilon\cos(r_0^2)}.$$

The right hand side oscillates an infinite number of times between $\frac{\pi}{1+\varepsilon}$ and $\frac{\pi}{1-\varepsilon}$ for r_0 in the interval $[0, \infty[$, and since $r_0 \mapsto r_0^2 + \varepsilon \sin(r_0^2)$ is a monotonically increasing function, also the function $h \mapsto T_\varepsilon(h)$ will oscillate an infinite number of times.

Data availability

No data was used for the research described in the article.

Acknowledgments

This work has been realized thanks to the Spanish AEI PID2019-104658GB-I00 grant; the Severo Ochoa and María de Maeztu Program for Centers and Units of Excellence in R&M CEX2020-001084-M grant; and the Catalan AGAUR 2021SGR00113 grant. Support was also received through FWO-NSFC bilateral grant G0F1822N.

We would like to thank the kind hospitality of the research team of Universitat de les Illes Balears who gave us the opportunity to work together for this work. This project was mainly carried out during a research visit of both authors to UIB. We would like to thank Armengol Gasull for his helpful discussions in some moments during the development of the work.

References

[1] X. Cen, New lower bound for the number of critical periods for planar polynomial systems, J. Differ. Equ. 271 (2021) 480–498.
[2] C. Chicone, M. Jacobs, Bifurcation of critical periods for plane vector fields, Trans. Am. Math. Soc. 312 (2) (1989) 433–486.
[3] A. Cima, A. Gasull, P.R. da Silva, On the number of critical periods for planar polynomial systems, Nonlinear Anal. 69 (7) (2008) 1889–1903.
[4] P. De Maesschalck, F. Dumortier, The period function of classical Liénard equations, J. Differ. Equ. 233 (2) (2007) 380–403.
[5] P. De Maesschalck, S. Rebollo-Perdomo, J. Torregrosa, Cyclicity of a fake saddle inside the quadratic vector fields, J. Differ. Equ. 258 (2) (2015) 588–620.
[6] W. Fulton, Algebraic Curves, Advanced Book Classics, Addison-Wesley Publishing Company, Advanced Book Program, Redwood City, CA, 1989, An introduction to algebraic geometry, Notes written with the collaboration of Richard Weiss, Reprint of 1969 original.
[7] A. Gasull, C. Liu, J. Yang, On the number of critical periods for planar polynomial systems of arbitrary degree, J. Differ. Equ. 249 (3) (2010) 684–692.
[8] A. Gasull, J. Yu, On the critical periods of perturbed isochronous centers, J. Differ. Equ. 244 (3) (2008) 696–715.
[9] M. Golubitsky, An introduction to catastrophe theory and its applications, SIAM Rev. 20 (2) (1978) 352–387.
[10] G.-M. Greuel, E. Shustin, Plane algebraic curves with prescribed singularities, in: Handbook of Geometry and Topology of Singularities II, Springer, Cham, 2021, pp. 67–122, ©2021.
[11] D. Marín, J. Villadelprat, The period function of generalized Loud's centers, J. Differ. Equ. 255 (10) (2013) 3071–3097.
[12] M. Sabatini, On the period function of Liénard systems, J. Differ. Equ. 152 (2) (1999) 467–487.